

Overdamped sine-Gordon kink in a thermal bath

Niurka R. Quintero* and Angel Sánchez†

Grupo Interdisciplinar de Sistemas Complicados (GISC), Departamento de Matemáticas, Universidad Carlos III de Madrid, Edificio Sabatini, Avenida de la Universidad 30, E-28911 Leganés, Madrid, Spain

Franz G. Mertens‡

Physikalisches Institut, Universität Bayreuth, D-95440 Bayreuth, Germany

(April 26, 2024)

We study the sine-Gordon kink diffusion at finite temperature in the overdamped limit. By means of a general perturbative approach, we calculate the first- and second-order (in temperature) contributions to the diffusion coefficient. We compare our analytical predictions with numerical simulations. The good agreement allows us to conclude that, up to temperatures where kink-antikink nucleation processes cannot be neglected, a diffusion constant linear and *quadratic* in temperature gives a very accurate description of the diffusive motion of the kink. The quadratic temperature dependence is shown to stem from the interaction with the phonons. In addition, we calculate and compute the average value $\langle \phi(x, t) \rangle$ of the wave function as a function of time and show that its width grows with \sqrt{t} . We discuss the interpretation of this finding and show that it arises from the dispersion of the kink center positions of individual realizations which all keep their width.

PACS: 03.40.Kf, 05.40.+j, 74.50.+r, 85.25.Cp

I. INTRODUCTION

There is no longer any controversy about the physical relevance of noise effects in spatially extended, nonlinear systems [1,2]: Indeed, the pervasive, joint role of nonlinearity and (static or dynamic) disorder has already been recognized in biophysics, electronics, optics, fluids, condensed matter, computational physics, etc. In most of these fields, nonlinear phenomena involve nonlinear coherent excitations, such as solitons or solitary waves, which play a key part in the corresponding system dynamics. It is because of this nowadays well established fact that much effort has been devoted to understand how stochastic perturbations affect solitons, mostly during the decade of the 80's (see [3–5] for reviews). In fact, early numerical simulations [6] already revealed that ϕ^4 solitary waves underwent Brownian-like motion in the presence of additive white noise, i.e., of thermal fluctuations. Subsequent works focused on the study of soliton diffusion, since it may be crucial in a number of problems, such as photoexcitation dynamics, photoconductivity of conducting polymers, or transport by phase solitons in charge-density-wave systems, to name a few [7].

Among the different soliton-bearing nonlinear models which have been studied in the above context, one which has received a great deal of attention is the sG equation. The interest in this model is both theoretical, as it displays the main features of more realistic and complicated cases while remaining analytically tractable, and applied, as it very approximately describes the dynamics of many physically relevant systems, such as one-dimensional (1D) magnets [8] or long Josephson junctions [9], for instance. Soliton diffusion governed by the sG (and other nonlinear Klein-Gordon equations) has been studied along two main, different lines which are discussed and compared, e.g., in Ref. [10]. The first one consists of considering extended excitations of the system (phonons) in equilibrium with both a single sG soliton and a heat bath at temperature T . This approach leads to two distinct diffusion regimes: anomalous diffusion, characterized by a diffusion constant proportional to T^2 , and viscous diffusion, when the appearance of a dynamical damping coefficient yields a diffusion constant proportional to T^{-1} . We will not follow this approach here; the interested reader is referred to the detailed review by Y. Wada [11]. The second manner is *à la Langevin*, i.e., introducing the influence of an external thermal bath by means of local fluctuations of the string and a local damping force related to that by an appropriate fluctuation-dissipation relationship. The corresponding equation of motion is then

$$\phi_{tt} - \phi_{xx} + \sin(\phi) = -\alpha\phi_t + \eta(x, t), \quad (1)$$

with

$$\langle \eta(x, t) \rangle = 0, \quad (2a)$$

$$\langle \eta(x, t)\eta(x', t') \rangle = D\delta(x - x')\delta(t - t'), \quad (2b)$$

where the diffusion coefficient $D = 2\alpha k_b T$, k_b being the Boltzmann constant, and $-\alpha\phi_t$ being the damping term with a dissipation coefficient α . This equation has been considered a number of times in the literature (see, e.g., [3] and references therein; see also [12] for related experimental work).

In this work, we focus on the Langevin version of the problem, with the aim of improving the analytical results obtained in the aforementioned works as well as of verifying them by numerical simulations specifically planned to that end. Furthermore, we concern ourselves with the overdamped limit of the sG equation, which reads

$$\alpha\phi_t - \phi_{xx} + \sin(\phi) = \epsilon\eta(x, t, \phi, \dots). \quad (3)$$

Note that we have introduced a factor ϵ in front of the noise term for convenience in the analytical calculations in section II. This equation (without noise, $\epsilon = 0$) was already considered by Eilenberger in [13], as the limit of the sG equation (1) in the case when the dissipation effect is strong enough in Eq. (1) and there is an input of energy into the system (see, e.g., [14,15] and references therein). On the other hand, Eq. (3), with additive noise as in (2), is interesting in itself: For example, it has been proposed as a model for crystal growth (see [16–18] and references therein). Equation (3) has also been studied to analyze the kink contribution to transport properties when the system is driven and thermally activated [16,19–21]. In particular, the work of Kaup [21] is the most closely related to the present one, as it presents a singular perturbation theory to compute the first-order (in T) correction to the kink mobility as well as the change of its shape. However, to our knowledge the free diffusion problem for the overdamped sG equation has not been addressed in the literature to date and, therefore, we believe that our results will be interesting by themselves. On the other hand, we also hope that what we learn in this case can be used towards obtaining a more complete, accurate picture of the full sG problem; we will discuss this question in the conclusions.

The outline of the paper is as follows: In section II, using a general perturbative method [13] which we recall in detail, we calculate the correlation functions of the position and the velocity of the kink center up to second-order in $k_b T$, as well as the diffusion coefficient and the mean value $\langle\phi(x, t)\rangle$ for fixed t . In section III we numerically integrate the stochastic partial differential equation (3), with noise given by Eq. (2), using the Heun scheme [22] and compute the time correlation function of the position of the kink center and the diffusion coefficient. We compare these results with the theoretical ones obtained in section II and find an excellent agreement. Finally, in section IV we discuss our results, summarize our main conclusions, and sketch lines for future research.

II. A GENERAL PERTURBATIVE APPROACH

Following the *Ansatz* proposed in [13,23], we assume that the solution of Eq. (3) can be expanded as

$$\phi(x, t) = \phi_0[x - X(t)] + \int_{-\infty}^{+\infty} dk A_k(t) f_k[x - X(t)], \quad (4)$$

where $f_k[x - X(t)]$ are the eigenfunctions of the linearized version of Eq. (3) [with $\epsilon = 0$], which along with $f_T[x - X(t)] = \frac{\partial\phi_0}{\partial x}[x - X(t)]$, form a complete set of orthogonal eigenfunctions (see Appendix I). The first term in the expansion (4) represents the translational mode related to the position of the kink center $X(t)$, whereas the second one characterizes the phonon modes (linear excitations around a kink) of the system. We will focus on the kink center motion as described by $X(t)$, as it is well established that such a particle-like picture is very generally enough to describe the behavior of the kink as a whole (X playing the rôle of a collective coordinate; see, e.g., [24] for a review).

In order to calculate the dynamics of the kink center, we begin by inserting (4) in (3), and projecting on the orthogonal basis [see Appendix I, relationships (36)] we obtain a system of differential equations for the unknown functions $X(t)$ and $A_k(t)$:

$$\begin{aligned} \dot{X}(t) &= -\frac{1}{8}\dot{X}(t) \int_{-\infty}^{+\infty} dk A_k(t) I_1(k) - \frac{1}{16\alpha} \int_{-\infty}^{+\infty} dk \int_{-\infty}^{+\infty} dk' A_k(t) A_{k'}(t) R_3(k, k') + \\ &+ \frac{\sqrt{D}}{8\alpha} \int_{-\infty}^{+\infty} f_T[x - X(t)] \eta(x, t) dx - \\ &- \frac{1}{48\alpha} \int_{-\infty}^{+\infty} dk \int_{-\infty}^{+\infty} dk_1 \int_{-\infty}^{+\infty} dk_2 A_k(t) A_{k_1}(t) A_{k_2}(t) R_6(k, k_1, k_2), \\ \frac{\partial A_k}{\partial t} + \frac{\omega_k^2}{\alpha} A_k(t) &= \dot{X}(t) \int_{-\infty}^{+\infty} dk A_k(t) I_3(k, k') + \frac{1}{2\alpha} \int_{-\infty}^{+\infty} dk \int_{-\infty}^{+\infty} dk' A_k(t) A_{k'}(t) R_4(k, k') - \end{aligned} \quad (5)$$

$$\begin{aligned}
& -\frac{\sqrt{D}}{\alpha} \int_{-\infty}^{+\infty} f_{k'}^*[x - X(t)] \eta(x, t) dx + \\
& + \frac{1}{6\alpha} \int_{-\infty}^{+\infty} dk \int_{-\infty}^{+\infty} dk_1 \int_{-\infty}^{+\infty} dk_2 A_k(t) A_{k_1}(t) A_{k_2}(t) R_7(k, k_1, k_2),
\end{aligned} \tag{6}$$

where

$$\begin{aligned}
I_1(k) &= \int_{-\infty}^{+\infty} \frac{\partial f_k}{\partial \theta} f_T(\theta) d\theta = \frac{i\pi\omega_k}{\sqrt{2\pi} \cosh\left(\frac{\pi k}{2}\right)}, \\
R_3(k, k') &= \int_{-\infty}^{+\infty} f_T(\theta) \frac{\partial f_T}{\partial \theta} f_k(\theta) f_{k'}^*(\theta) d\theta = -\frac{i(\omega_k^2 - \omega_{k'}^2)^2}{4\omega_k\omega_{k'} \sinh\left(\frac{\pi\Delta k}{2}\right)}, \quad \Delta k = k' - k, \\
I_3(k, k') &= \int_{-\infty}^{+\infty} \frac{\partial f_k}{\partial \theta} f_{k'}^*(\theta) d\theta, \\
R_4(k, k') &= \int_{-\infty}^{+\infty} [f_{k'}^*(\theta)]^2 \frac{\partial f_T}{\partial \theta} f_k(\theta) d\theta, \quad R_4(k, k) = \frac{3i\omega_k}{8\sqrt{2\pi} \cosh\left(\frac{\pi k}{2}\right)}, \\
R_6(k, k_1, k_2) &= \int_{-\infty}^{+\infty} \frac{\partial^2 f_T}{\partial \theta^2} f_k(\theta) f_{k_1}^*(\theta) f_{k_2}(\theta) d\theta, \\
R_7(k, k_1, k_2) &= \int_{-\infty}^{+\infty} \cos(\phi_0) f_{k'}^*(\theta) f_k(\theta) f_{k_1}^*(\theta) f_{k_2}(\theta) d\theta.
\end{aligned} \tag{7}$$

We now recall that, if we set $\epsilon = 0$ in (3), the static kink is an exact solution; hence, in what follows we will consider ϵ as a small perturbative parameter, and expand $A_k(t)$ and $X(t)$ in powers of ϵ . By substituting the series $A_k(t) = \sum_{n=1}^{\infty} \epsilon^n A_k^n(t)$ and $X(t) = \sum_{n=1}^{\infty} \epsilon^n X_n(t)$ in (5) and (6) we find a set of linear equations for the coefficients of these series. We only write down here the systems of equations up to order ϵ^3 , leaving out the cumbersome (albeit straightforward) equation for $A_k^3(t)$:

$O(\epsilon)$

$$\dot{X}_1(t) = \epsilon_1(t), \quad \langle \epsilon_1(t) \rangle = 0, \quad \langle \epsilon_1(t) \epsilon_1(t') \rangle = \frac{D}{8\alpha^2} \delta(t - t'), \tag{8a}$$

$$\frac{\partial A_k^1}{\partial t}(t) + \frac{\omega_k^2}{\alpha} A_k^1(t) = \frac{\epsilon_k(t)}{\alpha}, \quad \langle \epsilon_k(t) \rangle = 0, \quad \langle \epsilon_k(t) \epsilon_{k'}(t') \rangle = \frac{D}{\alpha^2} \delta(t - t') \delta(k - k'); \tag{8b}$$

$O(\epsilon^2)$

$$\begin{aligned}
\dot{X}_2(t) &= -\frac{\dot{X}_1(t)}{8} \int_{-\infty}^{+\infty} dk A_k^1(t) I_1(k) - \\
& - \frac{1}{16\alpha} \int_{-\infty}^{+\infty} dk \int_{-\infty}^{+\infty} dk' A_k^1(t) A_{k'}^1(t) R_3(k, k'),
\end{aligned} \tag{9a}$$

$$\begin{aligned}
\frac{\partial A_k^2}{\partial t}(t) + \frac{\omega_k^2}{\alpha} A_k^2(t) &= \dot{X}_1(t) \int_{-\infty}^{+\infty} dk A_k^1(t) I_3(k, k) + \\
& + \frac{1}{2\alpha} \int_{-\infty}^{+\infty} dk \int_{-\infty}^{+\infty} dk' A_k^1(t) A_{k'}^1(t) R_4(k, k');
\end{aligned} \tag{9b}$$

$O(\epsilon^3)$

$$\begin{aligned}
\dot{X}_3(t) &= -\frac{\dot{X}_1(t)}{8} \int_{-\infty}^{+\infty} dk A_k^2(t) I_1(k) - \frac{\dot{X}_2(t)}{8} \int_{-\infty}^{+\infty} dk A_k^1(t) I_1(k) - \\
& - \frac{1}{16\alpha} \int_{-\infty}^{+\infty} dk \int_{-\infty}^{+\infty} dk' A_k^2(t) A_{k'}^1(t) R_3(k, k') -
\end{aligned}$$

$$\begin{aligned}
& -\frac{1}{16\alpha} \int_{-\infty}^{+\infty} dk \int_{-\infty}^{+\infty} dk' A_k^1(t) A_{k'}^2(t) R_3(k, k') - \\
& -\frac{1}{48\alpha} \int_{-\infty}^{+\infty} dk \int_{-\infty}^{+\infty} dk_1 \int_{-\infty}^{+\infty} dk_2 A_k^1(t) A_{k_1}^1(t) A_{k_2}^1(t) R_6(k, k_1, k_2).
\end{aligned} \tag{10}$$

We now proceed with the first-order equations. The solutions of (8a) and (8b) can be written as

$$X_1(t) = \int_0^t \epsilon_1(\tau) d\tau, \quad A_k^1(t) = \exp\left(-\frac{\omega_k^2}{\alpha} t\right) \int_0^t \exp\left(\frac{\omega_k^2 \tau}{\alpha}\right) \epsilon_k(\tau) d\tau, \tag{11}$$

respectively. From these relations we can immediately compute averages over the quantities of interest, such as

$$\langle X_1(t) \rangle = 0, \quad \langle X_1(t) X_1(t') \rangle = \frac{D}{8\alpha^2} M, \tag{12}$$

$$\langle \dot{X}_1(t) \rangle = 0, \quad \langle \dot{X}_1(t) \dot{X}_1(t') \rangle = \frac{D}{8\alpha^2} \delta(t - t'), \tag{13}$$

$$\langle A_k^1(t) \rangle = 0, \quad \langle A_k^1(t) A_k^1(t') \rangle = \frac{D}{2\alpha\omega_k^2} \left[\exp\left(-\frac{\omega_k^2|t' - t|}{\alpha}\right) - \exp\left(-\frac{\omega_k^2(t + t')}{\alpha}\right) \right], \tag{14}$$

where $M = \min(t, t')$. For the next orders, the calculations are more involved but not difficult. After some tedious algebra, from Eqs. (9a)-(10) we find the average values of the position and velocity of the kink center

$$\langle X_2(t) \rangle = 0, \quad \langle \dot{X}_2(t) \rangle = 0, \tag{15}$$

$$\langle X_3(t) \rangle = 0, \quad \langle \dot{X}_3(t) \rangle = 0; \tag{16}$$

whereas it can be shown that, for large enough times,

$$\langle |A_k^2(t)| \rangle \sim \frac{3\sigma k_b T}{16\sqrt{2\pi}\omega_k^2}, \tag{17a}$$

$$\sigma = \int_{-\infty}^{+\infty} \frac{dk}{\omega_k \cosh\left(\frac{\pi k}{2}\right)} \approx 1.62386. \tag{17b}$$

The corresponding correlation functions for $X_2(t)$ and $\dot{X}_2(t)$ are

$$\langle X_2(t) X_2(t') \rangle = \frac{D^2 M}{512\alpha^3} + \frac{D^2 \pi}{4096\alpha^2} \int_{-\infty}^{+\infty} \frac{\left[\exp\left(-2\omega_k^2 M/\alpha\right) - 1 \right] dk}{\omega_k^2 \cosh^2\left(\frac{\pi k}{2}\right)}, \tag{18}$$

$$\begin{aligned}
\langle \dot{X}_2(t) \dot{X}_2(t') \rangle &= \langle \dot{X}_1(t) \dot{X}_1(t') \rangle \times \\
&\times \frac{D\pi}{256\alpha} \int_{-\infty}^{+\infty} \frac{\exp\left(-\omega_k^2|t' - t|/\alpha\right) - \exp\left(-\omega_k^2(t' + t)/\alpha\right) dk}{\cosh^2\left(\frac{\pi k}{2}\right)}.
\end{aligned} \tag{19}$$

Notice that the cross correlation function of $X_1(t)$ and $X_3(t)$ is of the same order as $\langle X_2(t) X_2(t') \rangle$, and also that $\langle X_1(t) X_2(t') \rangle = 0$. So, from Eqs. (8a) and (10) we have

$$\begin{aligned}
\langle X_3(t) X_1(t') \rangle &= \langle X_2(t) X_2(t') \rangle - \frac{D^2}{256\alpha^3} \int_{-\infty}^{+\infty} dk \ I_1(k) \times \\
&\times \left\{ \left(\int_{-\infty}^{+\infty} dm \frac{R_4(m, m)}{\omega_m^2} \right) \left[\frac{M}{\omega_k^2} + \frac{\alpha(\exp(-\omega_k^2 M/\alpha) - 1)}{\omega_k^4} \right] - \right. \\
&- \left. \int_{-\infty}^{+\infty} dn \frac{R_4(n, n)}{\omega_n^2} \frac{\alpha}{2\omega_n^2 - \omega_k^2} \left[\frac{(\exp(-2\omega_n^2 M/\alpha) - 1)}{2\omega_n^2} - \frac{(\exp(-\omega_k^2 M/\alpha) - 1)}{\omega_k^2} \right] \right\},
\end{aligned} \tag{20}$$

$$\begin{aligned} \langle \dot{X}_3(t) \dot{X}_1(t') \rangle &= -\frac{1}{8} \langle \dot{X}_1(t) \dot{X}_1(t') \rangle \times \\ &\times \int_{-\infty}^{+\infty} dk \left\{ \langle A_k^2(t) \rangle I_1(k) - \frac{1}{8} \langle [A_k^1(t)]^2 \rangle |I_1(k)|^2 \right\}. \end{aligned} \quad (21)$$

Finally, from (13), (19) and (21) we obtain the final result, namely that for large t [i.e., taking the limit $t \rightarrow \infty$ in Eqs. (19) and (21) in all terms except those related to $X_1(t)$] the correlation function $\langle \dot{X}(t) \dot{X}(t') \rangle$ is given up to order ϵ^4 by

$$\begin{aligned} \langle \dot{X}(t) \dot{X}(t') \rangle &= \epsilon^2 \langle \dot{X}_1(t) \dot{X}_1(t') \rangle + \\ &+ \epsilon^4 (\langle \dot{X}_2(t) \dot{X}_2(t') \rangle + \langle \dot{X}_1(t) \dot{X}_3(t') \rangle + \langle \dot{X}_3(t) \dot{X}_1(t') \rangle) + \dots \\ &= \frac{\epsilon^2}{8} \langle \dot{X}_1(t) \dot{X}_1(t') \rangle \left\{ 1 + \epsilon^2 \left(\frac{3}{32} + \frac{3}{128} \sigma^2 \right) k_b T \right\} + o(\epsilon^4). \end{aligned} \quad (22)$$

We now return to our original equation notation: We set ϵ equal to one and consider $\sqrt{k_b T}$ as the small parameter. When t goes to infinity and imposing $\epsilon = 1$, from Eqs. (12), (18) and (20) we find

$$\langle [X(t)]^2 \rangle = \frac{k_b T}{4\alpha} t \left\{ 1 + \left(\frac{3}{32} + \frac{3}{128} \sigma^2 \right) k_b T \right\}. \quad (23)$$

Note that the slope of this function is the kink diffusion coefficient, so if one takes into account the second-order correction one obtains that the diffusion coefficient is a quadratic function of the temperature. We postpone our comments to Sec. IV, where a comparison with the previously available results will be made.

To complete this work, we can calculate in a very simple way the average value of the wave function $\phi(x, t)$ in first order: From Eq. (4) we have that

$$\langle \phi(x, t) \rangle = \langle \phi_0[x - \epsilon X_1(t)] \rangle + O(\epsilon^2). \quad (24)$$

In this last relation we have taken into account that $\langle A_k(t) \rangle = \epsilon \langle A_k^1(t) \rangle + O(\epsilon^2)$ and $\langle A_k^1(t) \rangle = 0$ [see Eq. (14)].

If we solve the corresponding Fokker-Planck equation for X_1 [see Eq. (8a)], we obtain that the probability distribution function for X_1 is a Gaussian function given by

$$p(X_1) = \sqrt{\frac{4\alpha^2}{\pi t D}} \exp \left(-\frac{4\alpha^2 X_1^2}{D t} \right). \quad (25)$$

So, one can define the average value $\langle \phi(x, t) \rangle$ as

$$\langle \phi(x, t) \rangle = \int_{-\infty}^{+\infty} dX_1 p(X_1) \phi_0[x - \epsilon X_1(t)]. \quad (26)$$

Unfortunately we have not found the analytical expression for this integral. But we have calculated it numerically, and below we will compare it to the simulations for the full partial differential equation.

III. NUMERICAL SIMULATIONS

For our numerical simulations of the partial differential equation (3), we have used the Heun method [22], whose stochastic properties are well known and suitable for comparison to our theoretical predictions. We numerically integrate Eqs. (3), with white noise (2), starting from an unperturbed kink at rest and taking the average values over 1000 realizations. The other parameters are $\alpha = 1$, $\Delta x = 0.05$, and $\Delta t = 0.001$. In the evaluation of the simulations, we have defined the center of the kink as follows: We first find all the lattice points i such that $\phi_i \leq \pi$ and $\phi_{i+1} \geq \pi$ or vice versa. We then interpolate to obtain the points x_i where the field ϕ crosses π . In case that, due to the noise-induced deformation of the kink, there is more than one such x_i , we average them to finally obtain the numerical kink center position, x_c . As discussed below, this introduces some error, but other alternatives we tested (such as the center of mass, for instance) gave results which did not really represent the kink location, and moreover its calculation from numerics is much less accurate. Once the center is obtained, we computed also its variance $\langle [X(t)]^2 \rangle$.

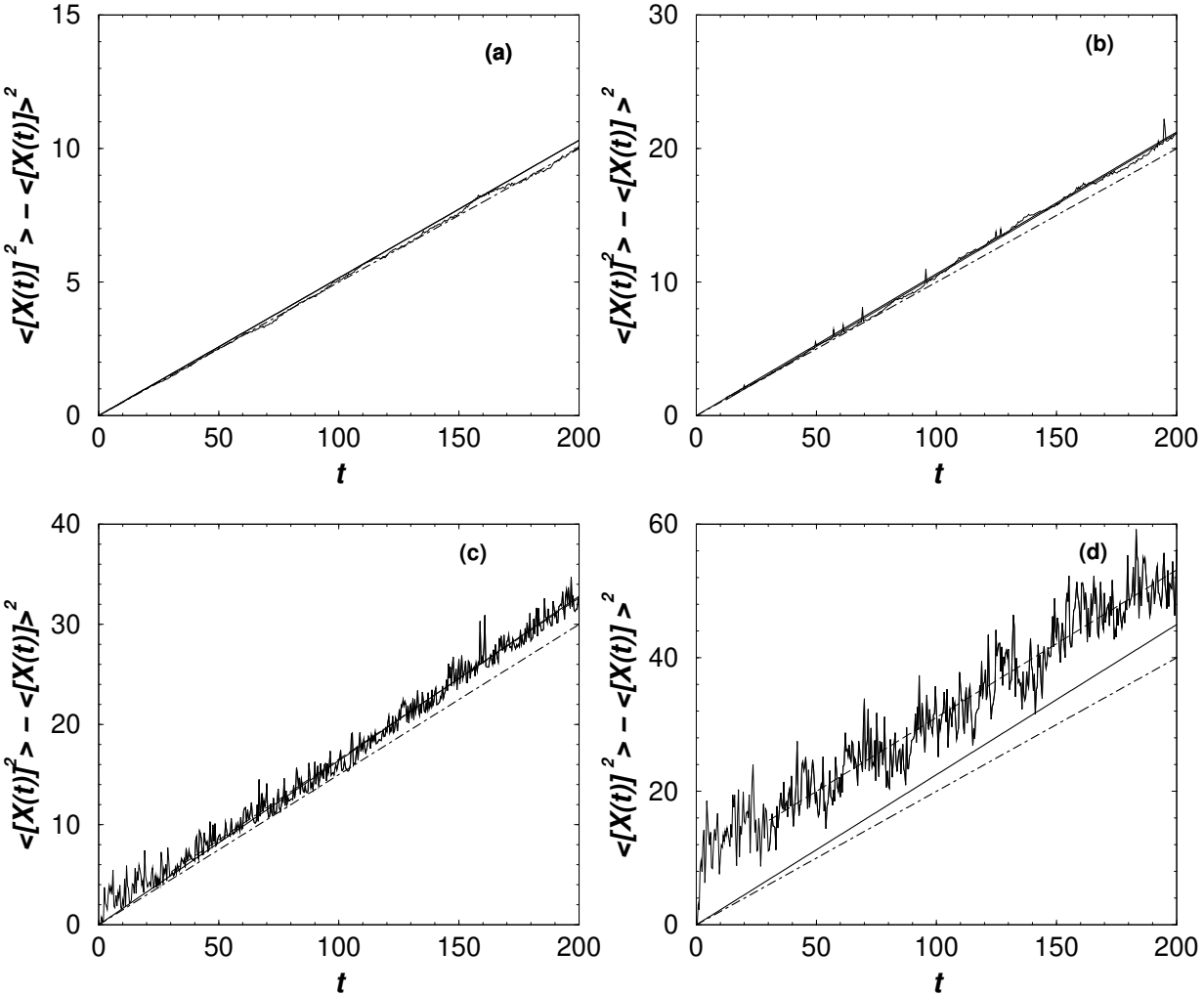


FIG. 1. Simulations with initial condition given by a static kink initially located at $X(0) = 0$, and subject to a thermal bath. As a continuous (but wiggly) line, we have plotted $\langle [X(t)]^2 \rangle$ as obtained by numerical integration of Eq. (3) for (a) $k_b T = 0.2$, (b) $k_b T = 0.4$, (c) $k_b T = 0.6$ and (d) $k_b T = 0.8$. Overimposed to these lines the linear regression of the numerical results for $t \geq 30$ is shown (long-dashed line). The solid line is the theoretical prediction $\langle [X(t)]^2 \rangle$ from Eq. (23); this line practically overlaps with the linear regression in Fig. a, b, and c. The first-order result $\langle [X(t)]^2 \rangle$ from Eq. (12) is shown as a dot-dash line.

Figures 1(a)-(d) show a comparison of our numerical results with the analytical predictions, Eqs. (12) and (23), for different values of $k_b T$. We see that there is an excellent agreement between theory and numerics except for the highest value of $k_b T$ [Fig. 1(d)]. We have checked that this disagreement arises from the way we compute the kink center: For such large values of the noise, points where $\phi(x, t) = \pi$ are found all over the system, irrespective of their distance to the kink center (we note, however, that the temperature was not high enough to create new kink-antikink pairs). Those points contribute to the center position through our averaging procedure, and in fact their contribution can be shown to be additive, i.e., it amounts to move the whole curve $\langle [X(t)]^2 \rangle$ upwards. This is indeed what occurs in Fig. 1(d), and as we will see below the slope is very close to the predicted one. The same behavior is found for higher temperatures in so far no new kinks are created (not shown). Interestingly, a first conclusion that can be drawn from these figures is that already for not so high temperatures, $k_b T \geq 0.4$, as time passes the kink behavior becomes more and more different from the first-order prediction, showing clearly the necessity for the second-order correction.

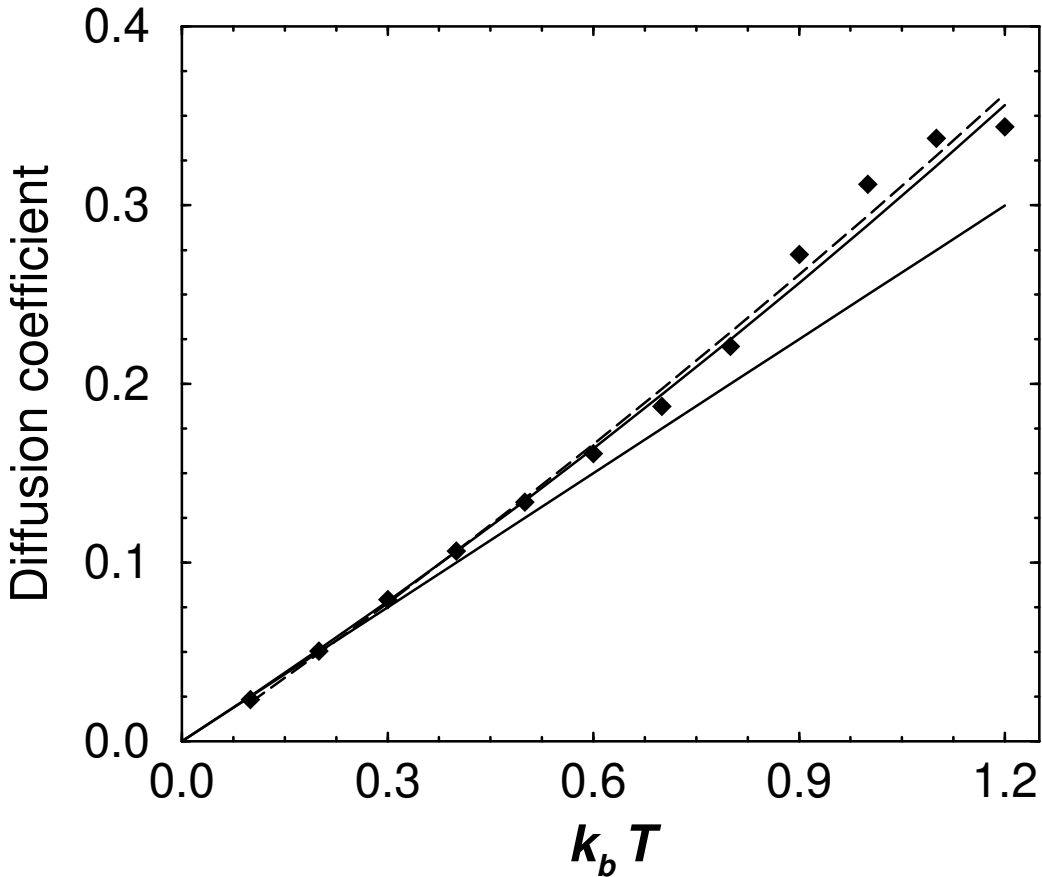


FIG. 2. Lower solid line: the function D_1 ; upper solid line: D_2 , which represent the first- and second-order results for the kink diffusion coefficient [see Eqs. (12) and (23)]. Diamonds represent the numerical values of the kink diffusion coefficient, obtained by numerical integration of Eq. (3) with final time $t_f = 200$ (as in Fig. 1) and different values of $k_b T$. A quadratic regression of these numerical values is also plotted (long-dashed line).

We have calculated the numerical values of the diffusion coefficient for several temperatures by taking the slope of $\langle [X(t)]^2 \rangle$, which we obtain from a linear fit of the data for not so early times ($t \geq 30$) to avoid transient effects coming from the adjustment of the kink to the heat bath. Note also that our prediction for the second-order contribution was obtained in the large-time limit, so we should not try to fit the whole evolution. The figures also show those linear regressions. Subsequently, in Fig. 2 we have compared the computed slopes with the first and second-order coefficients $D_1 = \frac{k_b T}{4\alpha}$, and $D_2 = \frac{k_b T}{4\alpha} \left\{ 1 + \left(\frac{3}{32} + \frac{3}{128} \sigma^2 \right) k_b T \right\}$ [see. Eqs. (12) and (23)]. The comparison is once again very good, and points out very clearly that for values of $k_b T$ as low as 0.3, the first-order prediction begins to deviate from the diffusion constant measured in the simulations. In addition, the quadratic fit to the simulation results, shown as a long-dashed line in Fig. 2, practically coincides with the second-order prediction in the whole studied range.

As a final verification of our results, in Fig. 3 we have plotted the mean value $\langle \phi(x, t) \rangle$ of the wave function at three different times along its evolution, both as obtained from the numerical simulation of the partial differential equation and from the numerical evaluation of Eq. (26). The perfect agreement between these expressions provides us with a hint to derive an approximate analytical estimate of the evolution of $\langle \phi \rangle$ from the integral (26). From Fig. 3 one immediately concludes that the width of $\langle \phi \rangle$ increases with temperature and time. Let us define the width of $\langle \phi \rangle$ by

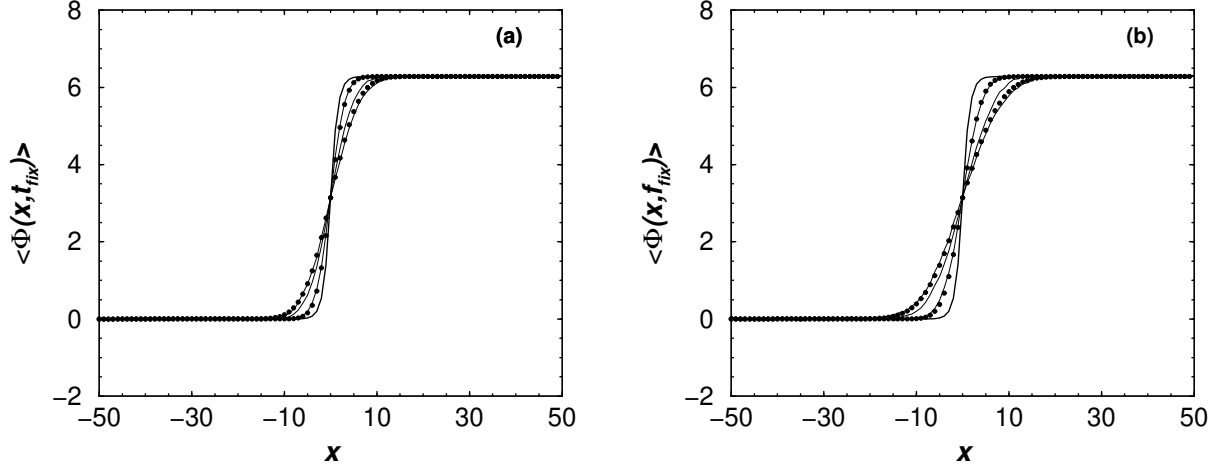


FIG. 3. Solid lines: Snapshots of the evolution of $\langle \phi(x, t) \rangle$, obtained from numerical simulations of the partial differential equation, for fixed times 40, 120 and 200, respectively. The initial kink (unperturbed, at rest, is also included for comparison). The width of $\langle \phi \rangle$ increases as time progresses. The overimposed points have been computed numerically from the integral (26). Plots correspond to $k_b T = 0.4$ (a), and 0.8 (b); the width of $\langle \phi \rangle$ is seen to increase also with temperature.

$$L(t) = \sqrt{\frac{\int_{-\infty}^{+\infty} x^2 \langle [\phi_x(x, t)]^2 \rangle dx}{\int_{-\infty}^{+\infty} \langle [\phi_x(x, t)]^2 \rangle dx}}. \quad (27)$$

With this definition, we can now calculate $\langle [\phi_x(x, t)]^2 \rangle$ by using the distribution function of $X_1(t)$; this procedure yields

$$L(t) \approx \sqrt{L_0^2 + \langle [X_1(t)]^2 \rangle}, \quad (28)$$

$$\text{where } L_0^2 = \frac{\int_{-\infty}^{+\infty} dx \ [x^2 / \cosh^2(x)]}{\int_{-\infty}^{+\infty} dx \ [1 / \cosh^2(x)]} = 0.8225.$$

It is important to note that, of course, we could define $L(t)$ using $\langle \phi_x(x, t) \rangle$ instead of $\langle [\phi_x(x, t)]^2 \rangle$ in the above expression, or equivalently another quantity which is localized around the kink center. However, as all possible (and sensible) definitions of $L(t)$ give more or less the same results, the difference between them becomes a constant factor when $\langle [X_1(t)]^2 \rangle$ increases above L_0^2 (for example, for large enough t). So, we expect that the ratio

$$\frac{L(t)}{L(t_{fix})} \rightarrow \sqrt{\frac{t}{t_{fix}}}, \quad (29)$$

for large enough t and t_{fix} .

Figure 4 shows a comparison of this prediction with the numerical evaluation of the width of $\langle \phi \rangle$ from Eq. (26). From these plots we see that the broadening of $\langle \phi \rangle$ behaves indeed as \sqrt{t} : We can compare the analytical slope equal to 0.5 with the numerical ones equal to 0.4276 and 0.4517 for plots (a) and (b) respectively. The slope in (b) is closer to the analytical value due to the fact that t_{fix} is larger than in case (a), which agrees with the above considerations.

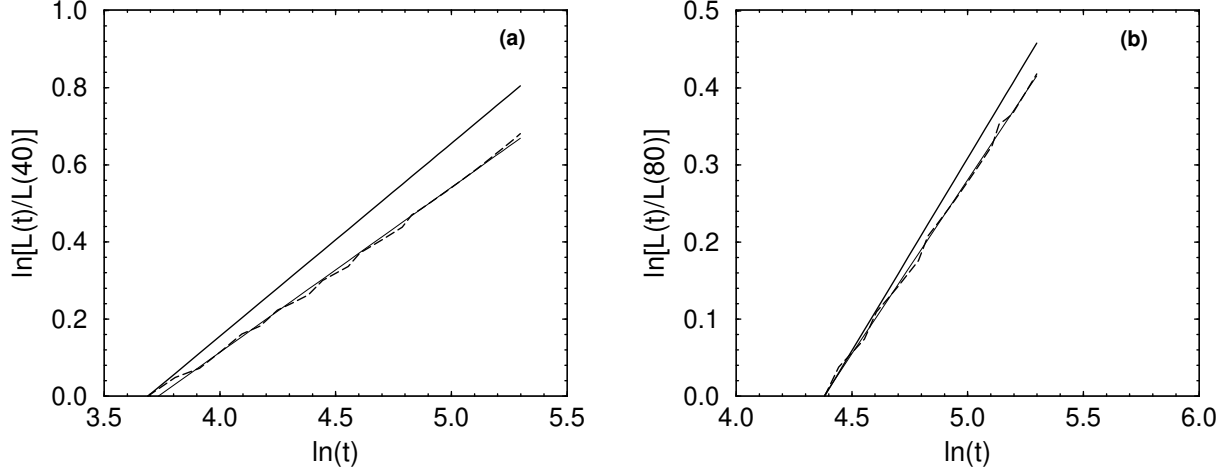


FIG. 4. Solid lines: Analytical values of $\ln[L(t)/L(t_{fix})]$ for $t_{fix} = 40$ (a) and $t_{fix} = 80$ (b). In both cases $\alpha = 1$ and $k_b T = 0.6$. Long-dashed lines: numerical values, calculated from (26). The solid lines over the long-dashed ones correspond to the linear regression of the numerical points.

IV. DISCUSSION AND CONCLUSIONS

As we have seen in the previous section, our second-order theoretical predictions constitute a very accurate description of the kink dynamics for a wide range of temperatures, up to a value of $k_b T \simeq 1$. In fact, the range of validity of the analytical results might be somewhat higher, provided a better way to estimate the kink center from the numerical simulations could be devised. In any event, the occurrence of π -crossings far away from the kink center for values around $k_b T \simeq 1$ indicates that further increments of the temperature would undoubtedly produce kink-antikink pairs, thus invalidating our collective coordinate approach which necessarily relies on the identification of the individual kink propagation. We note that this value is a little over 10% of the kink rest mass ($M_0 = 8$ in our units); in this respect, a similar result was obtained in [25] for the overdamped ϕ^4 model by means of a similar perturbative approach (with the caveat that the numerical data presented in [25] only allow one to guess what is the range of validity of their results).

It is interesting to pursue further the comparison of the results for the sG and ϕ^4 cases. In our calculations for sG, we have found that the second-order correction is clearly smaller (albeit relevant) than the first-order one. The structure of the perturbative calculation allows to identify the origin of that correction: It comes from the interaction of the phonons (described by the functions A_k) with the kink. Now, in the ϕ^4 case, the situation is quite different: Indeed, the second-order correction is much *larger* than the one we find here, and the reason is the so-called internal mode, present for ϕ^4 kinks and absent in the sG case. The coupling between this internal mode (which has been shown to act as a reservoir of energy available for exchange with the kink translation mode [26]) and the kink motion can be shown, by a careful examination of the calculation in [25], to be responsible for most of the second-order correction, while the phonons produce a second-order term comparable to the one we have found. We thus see that, while the range of validity of the analytical approach is in principle the same in both cases, the physics is certainly different, and in fact the question arises as to the validity of this kind of perturbative calculation for the ϕ^4 problem in view of the large contribution of the internal mode. This is an interesting question that deserves further analytical and numerical work.

Coming back to our results for the sG kink, the fact that the second-order correction is smaller than the first-order term makes us confident that our expansion is likely to be free of problems coming from secular terms. This belief is reinforced by the result that, up to the validity range discussed above and limited by kink-antikink creation phenomena, the second-order result describes very accurately the kink behavior, which deviates very little from the predicted diffusive motion. It is then reasonable to expect higher-order contributions (whose calculation is extremely cumbersome, but feasible in principle) to be negligible, thus yielding our theoretical result as the final one for the kink

diffusion in the overdamped sG problem. In this context, it is also important to realize that Eqs. (8a)-(8b), which are only first-order, can also be obtained following the McLaughlin and Scott procedure [27] (see also [24]). However, the advantages of the perturbative scheme we have used are, on one hand, that we were able to obtain the next order in the expansion, and on the other hand, we demonstrated that the second order originates in the interaction between phonon and translational modes of the sG kink.

A final remark on our results relates to the mean value of the wave function $\langle \phi(x, t) \rangle$ as a function of t , that must *not* be interpreted as the shape of the kink; in contrast to the interpretation in [25]. We first note that the width of the kink cannot increase from its value when unperturbed at rest; the sG equation, being Lorentz invariant, implies that the kink width diminishes when in motion, and therefore an increasing of the width would be very difficult to understand on physical grounds. Indeed that is not the case. The broadening of the mean wave function comes in fact from the dispersion of the individual realizations, as is immediately seen from Fig. 5. As may be seen all individual realizations show a width comparable to the initial kink width, which agrees with our physical intuition. The observed \sqrt{t} behavior, discussed at the end of the preceding section, is then evidently related to the fact that the variance of the kink position has that behavior too. The correct interpretation of the width of $\langle \phi(x, t) \rangle$ is that it represents the area in which the kink can be located as its diffusive motion progresses. A similar result has been found for multiplicative noise in [28] (see also [2] and references therein).

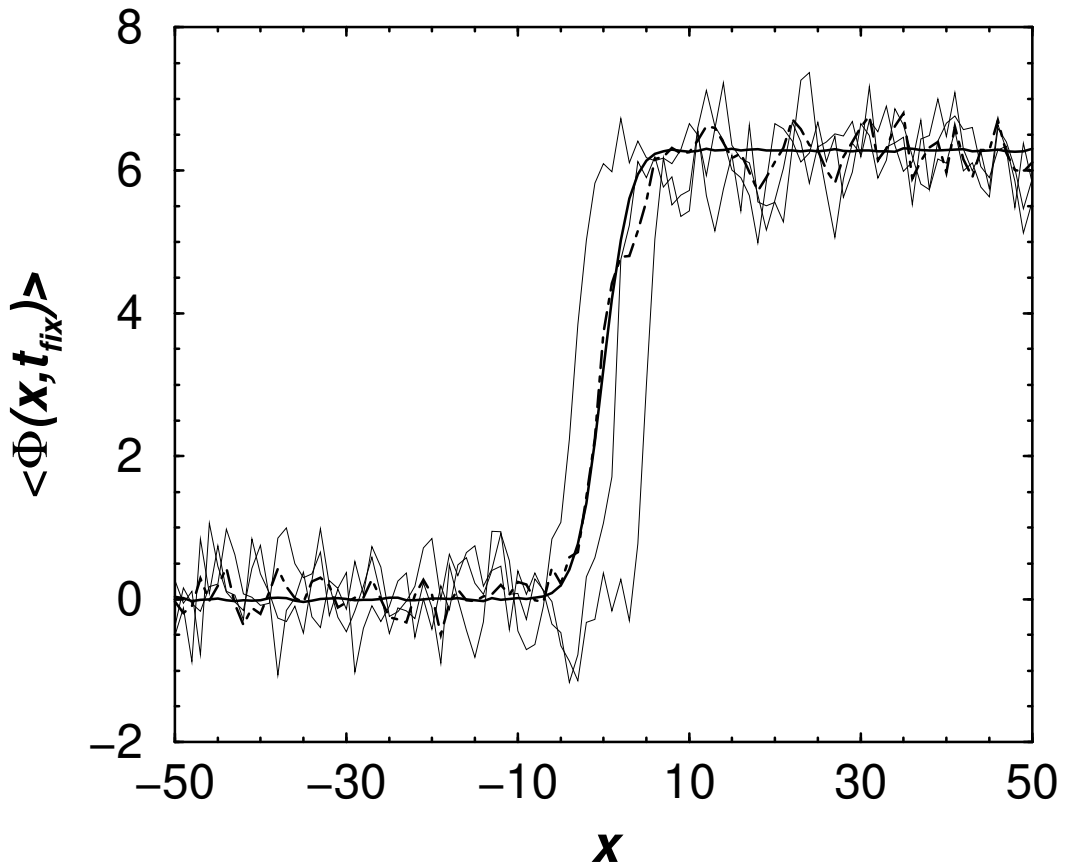


FIG. 5. Average of the wave function for $k_b T = 0.4$ and $t = 200$ obtained from 1000 realizations (wider solid line), compared to the average of only 5 realizations (dot-dashed line). Also represented are 3 of these individual realizations. Note the different slope and width of the average values as compared to individual realizations.

To conclude, we want to stress that our main result is the quadratic dependence of the diffusion constant on the temperature, stemming from the kink-phonon interactions. This has been verified numerically to a high degree of accuracy. We have carried out standard Langevin dynamics simulations following a well grounded procedure, the Heun method, as far as statistical properties are concerned [22]. We can thus be sure that what we are dealing with is indeed the dynamics of a sG kink at finite temperature. Therefore, our analytical calculations and our numerical simulations establish firmly the quadratic dependence of the kink diffusion constant on the temperature for the first time. Now the question remains as to the behavior of *underdamped* sG kinks. Preliminary calculations [29] seem to indicate that for underdamped sG kinks the second-order correction is of the same order as that found here, which would support the applicability of the previous calculations at least for small temperatures and not too small damping. To date, no detailed comparison with numerical simulations has ever been done to check the importance of the second-order correction. On the other hand, it would be interesting to compare the results of our approach with the theoretical analysis and experiments in [12]. Such comparison would provide much insight into the importance of second and higher-order corrections in actual physical systems. Work along these lines is in progress [29]

ACKNOWLEDGEMENT

We are grateful to Esteban Moro, Grant Lythe, and José María Sancho for discussions. Work at GISC (Leganés) has been supported by CICYT (Spain) grant MAT95-0325 and DGES (Spain) grant PB96-0119. Travel between Bayreuth and Madrid is supported by “Acciones Integradas Hispano-Alemanas”, a joint program of DAAD (Az. 314-AI) and DGES. This research is part of a project supported by NATO grant CRG 971090.

Note added in proof: After acceptance of this paper, we have implemented an improved algorithm for detecting the kink center in our code. With this new procedure, no spurious contributions (see discussion below Fig. 1) to the variance appear: Specifically, Fig. 1(d) is largely improved, and the numerical results overlap the theoretical prediction, thus confirming the interpretation we have provided of the discrepancy. A detailed report will be given in [29].

APPENDIX I

One class of solutions of (3) [with $\epsilon = 0$] is represented by a static kink

$$\phi_0(x, t) = 4 \arctan[\exp(x)]. \quad (30)$$

The perturbations over this equation may be treated by assuming that the solution of (3) [with $\epsilon = 0$] has the form

$$\phi(x, t) = \phi_0(x) + \psi(x, t), \quad \psi(x, t) \ll \phi_0(x). \quad (31)$$

If we substitute Eq. (31) in (3) [with $\epsilon = 0$] and linearize around $\phi_0(x)$, we obtain the following equation for $\psi(x, t)$

$$\alpha\psi_t = \psi_{xx} - \left[1 - \frac{2}{\cosh^2(x)}\right]\psi. \quad (32)$$

Then, the solution of (32) may be written as $\psi(x, t) = f_k(x) \exp\left(-\frac{\omega_k^2 t}{\alpha}\right)$, where $f_k(x)$ satisfies the eigenvalue problem given by

$$-\frac{\partial^2 f_k}{\partial x^2} + \left[1 - \frac{2}{\cosh^2(x)}\right]f_k = \omega_k^2 f_k. \quad (33)$$

This equation admits the following eigenfunctions with their respective eigenvalues

$$f_T(x) = \frac{2}{\cosh(x)}, \quad \omega_T^2 = 0, \quad (34)$$

$$f_k(x) = \frac{\exp(ikx) [k + i\tanh(x)]}{\sqrt{2\pi} \omega_k}, \quad \omega_k^2 = 1 + k^2. \quad (35)$$

Notice, that $f_T(x)$ and $f_k(x)$ form a complete set of functions with the orthogonality relations

$$\int_{-\infty}^{+\infty} f_T^2(x) dx = 8, \quad \int_{-\infty}^{+\infty} f_T(x) f_k(x) dx = 0, \quad (36a)$$

$$\int_{-\infty}^{+\infty} f_k(x) f_{k'}^*(x) dx = \delta(k - k'). \quad (36b)$$

* kinter@math.uc3m.es

† anxo@math.uc3m.es

‡ franz.mertens@theo.phy.uni-bayreuth.de

- [1] *Fluctuation phenomena: Disorder and nonlinearity*, edited by A. R. Bishop, S. Jiménez, and L. Vázquez (World Scientific, Singapore, 1995).
- [2] J. García-Ojalvo and J. M. Sancho, *Noise in spatially extended systems* (Springer, New York, 1999).
- [3] F. G. Bass, Yu. S. Kivshar, V. V. Konotop, and Yu. A. Sinitzyn, Phys. Rep. **157**, 63 (1988).
- [4] A. Sánchez and L. Vázquez, Int. J. Mod. Phys. B **5**, 2825 (1991).
- [5] V. V. Konotop and L. Vázquez, *Nonlinear random waves* (World Scientific, Singapore, 1994).
- [6] T. R. Koehler, A. R. Bishop, J. A. Krumhansl, and J. R. Schrieffer, Solid State Commun. **17**, 1515 (1975).
- [7] Yu Lu, *Solitons and polarons in conducting polymers* (World Scientific, Singapore, 1988); G. Gruner, *Density waves in solids* (Addison-Wesley, New York, 1994).
- [8] H. J. Mikeska, J. Phys. C **11**, 129 (1978).
- [9] A. Barone and G. Paternó, *Physics and applications of the Josephson effect* (Wiley, New York, 1982).
- [10] B. A. Ivanov and A. Kolezhuk, Phys. Lett. A **146**, 190 (1990).
- [11] Y. Wada, Prog. Theo. Phys. Suppl. **113**, 1 (1993).
- [12] M. G. Castellano, G. Torrioli, C. Cosmelli, A. Costantini, F. Chiarello, P. Carelli, G. Rotoli, M. Cirillo and R. L. Kautz, Phys. Rev. B **54**, 15417 (1996).
- [13] G. Eilenberger, Z. Physik B **27**, 199 (1977).
- [14] Yu. S. Kivshar, and B. A. Malomed, Rev. Mod. Phys. **61**, 763 (1989).
- [15] C. H. Bennett, M. Büttiker, R. Landauer, and H. Thomas, J. Stat. Phys. **24**, 419 (1981).
- [16] J. Krug and H. Spohn, Europhys. Lett. **8**, 219 (1989).
- [17] A. Sánchez, D. Cai, N. Grønbech-Jensen, A. R. Bishop, and Z. J. Wang, Phys. Rev. B **51**, 14 664 (1995).
- [18] R. Rangel and L. E. Guerrero, Fractals **3**, 533 (1995).
- [19] M. Büttiker, and R. Landauer, J. Phys. C, **13**, L325 (1980).
- [20] M. Büttiker, and R. Landauer, Phys. Rev. A **23**, 1397 (1981).
- [21] D. J. Kaup, Phys. Rev. B **27**, 6787 (1983).
- [22] Stochastic effects in Physical Systems, M. San Miguel, and R. Toral, *Instabilities and Nonequilibrium Structures*, (V Ed. E, Tirapegui, W. Zeller, Kluwer, 1997).
- [23] R. Rajaraman, *Solitons and Instantons* (North-Holland Publishing Company, Amsterdam, 1982).
- [24] A. Sánchez and A. R. Bishop, SIAM Rev. **40**, 579, (1998).
- [25] Jacek Dziarmaga and Wojtek Zakrzewski, preprint [cond-mat/9802039](http://arxiv.org/abs/cond-mat/9802039).
- [26] D. K. Campbell, J. F. Schonfeld and C. A. Wingate, Physica D **9**, 1 (1983).
- [27] D. W. McLaughlin and A. C. Scott, Phys. Rev. A **18**, 1652 (1978).
- [28] J. Armero, J. M. Sancho, J. Casademunt, A. M. Lacasta, L. Ramírez-Piscina, and F. Sagués, Phys. Rev. Lett. **76**, 3045 (1996).
- [29] N. R. Quintero, A. Sánchez, and F. Mertens, unpublished.